MEDWIN PUBLISHERS
Committed to Create Value for Researchers

Cytology & Histology International Journal
ISSN: 2642-116X

MMP-9 Expression in Normal Rabbit Chondrocytes

Hanan H. Abd-Elhafeez[1]*, Basma Kamal[2], Abeera M. El-Sayed[3] and Soha A. Soliman[4]

[1]Department of Anatomy, Embryology and Histology, Assiut University, Egypt
[2]Department of Anatomy and Embryology, University of Sadat City, Egypt
[3]Fellow of Sohag University Hospital, Sohag University, Egypt
[4]Department of Histology, South Valley University, Egypt

Research Article
Volume 5 Issue 1
Received Date: April 08, 2021
Published Date: April 29, 2021

***Corresponding author:** Hanan H Abd Elhafeez, Department of Anatomy, Embryology and Histology, Assiut University, Assiut, Egypt, Email: hhnnzz91@aun.edu.eg

Abstract

Chondrocytes regulate anabolic and catabolic processes to maintain the extracellular matrix components. Catabolic activities depend on the proteolytic action of the matrix -degrading enzymes including ADAMTS (A disintegrin and metalloproteinases) and MMP (Matrix Metalloproteinase). The current study explored the distribution of MMP-9 in normal articular cartilages of the embryos rabbit. Articular cartilage has grown by appositional growth that the perichondrial stem cells differentiate into chondrocytes. MMP-9 positive perichondrial stem cells or chondroblasts and early chondrocytes. Mature chondrocytes exhibited weak immunoaffinity for MMP-9. In conclusion, MMP-9 was essential during chondrocytes growth. The current study alludes to the potential role of MMP-9 during the growth of the articular cartilage.

Keywords: MMP-9; Chondrocytes; Chondroblasts; Rabbit; Femur

Abbreviations: MMP: Matrix Metalloproteinase; ADAMTS: A Disintegrin And Metalloproteinases; ABC: Avidin-Biotin Complex; DAB: Diaminobenzidine.

Introduction

Chondrocytes are derived from mesenchymal stem cells. They have genotypic characteristics that are devoted to the synthesis, and turnover of extracellular cartilage matrix to maintain a proper function of the specific tissue. Chondrocytes secret Type II collagen and proteoglycans that provide the cartilage matrix with unique biomechanical properties. Tissue homeostasis is a balanced process between cell death and propagation. Cartilage turnover depends on the division of the chondrocytes or differentiation of the chondroblasts. The chondroblasts or perichondrial stem cells are actively dividing cells. They had a chondrogenic potential that activates to form a cartilage matrix. They are contribute to the appositional growth of the cartilage.

Chondrocytes regulate anabolic and catabolic processes to maintain the extracellular matrix components [1]. Proteoglycans undergo rapid remodeling whereas collagen repair is complicated. Proteoglycans degradation occurs through aggrecanases or ADAMTS (A disintegrin and metalloproteinases) including ADAMTS-4 and ADAMTS-5 [1,2]. Collagen is specifically degraded by members of the matrix metalloproteinase (MMP) family including MMP-1, MMP-2, MMP-8, MMP-13 and MMP-14 [3]. Uncontrolled proteolytic activities of chondrocytes cause arthritic cartilage. Several members of MMP and ADAMs contribute to cartilage degradation during arthritis. MMP-9 or gelatinase B is expressed in both normal adult human and osteoarthritic chondrocytes [4]. The current study explored

the distribution of MMP-9 in normal articular cartilages of the embryos rabbit.

Material and Methods

Ethical Statements:

The Ethics Committee of Scientific Research on experimental animals, Faculty of Veterinary Medicine, Assiut University, and South Valley University, Egypt, approved all procedures used in the study.

Sample Collection:

Apparently healthy adult female rabbit, the New Zealand white rabbits (Oryctolagus cuniculus), obtained from the farm of the Faculty of Agriculture, South Valley University, Qena, Egypt. Adult healthy male rabbits fertilized female rabbits. The day of mating is considered the zero-day of pregnancy. We detected the pregnant does by ultrasonography. Seven rabbit embryos were collected at 24 days of gestation after euthanization of the pregnant rabbits. The femur bones of the rabbit's embryos were dissected.

Sample Fixation and Decalcification:

Fixation: Femur fixed after cutting longitudinally in Worbel-Moustafa fixative Wrobel & Moustafa [5], Moustafa, et al. [6], Abd Elhafeez, et al. [7], Abd Elhafeez, et al. [8], Abdel latief Soliman & Ali Emeish [9] for 24 hours at 4°C. Then transfer the bone sample into 70% ethanol alcohol for another 24hr at 4°C.

Decalcification: Femur decalcified for light microscopy by using a 5% 5% EDTA (in 0.1 M Tris/HCl buffer, pH 7.4) Roach [10] for 20 days and change the EDTA solution every 5-6 days until the bone becomes soft. They were washed 4 times for 15 minutes in 0.1 M sodium phosphate buffer (pH 7.2) (Table 1) showing the components of buffers). All components of buffers were cited in Bancroft's Theory and Practice of Histological Techniques [11].

Fixative	Components	Amount
Wrobel-Moustafa-Fixative	Paraformaldehyde, 25% freshly prepared 40 ml	40 ml
	Phosphate buffer (0.2 M, pH 7.4) 125 ml	125 ml
	Saturated picric acid 37.5 ml	37.5 ml
	Calcium chloride 0.5 mg	0.5 mg
Na-Phosphate buffer (0.1 M, pH 7.4)	Solution A	
	Na2HPO4 2H2O	17.02 g
	Distilled water	600 ml
	Solution B	
	NaH2PO4 H2	6 g
	Distilled water	200 ml
	Using solution	
	Solution A	580 ml
	Solution B	219 ml
Tris-HCL buffer pH 7.4	Solution A	
	Tris	2.42 g
	Distilled water	100 ml
	Solution B	
	HCL	1.7 ml
	Distilled water	100 ml
	Using solution	
	Solution A	25ml
	Solution B	20.7 ml
	Distilled water	Complete until 100 ml

Citrate-buffer (pH 6.0)	Solution A	
	CitrateC6H8O7 H2O	21 g
	Distilled water	1 liter
	Solution B	
	Sodium citrateNa3C6H5O7 2H2O	29.41 g
	Distilled water	1 liter
	Using solution	
	Solution A	9 ml
	Solution B	41 ml
	Distilled water	Add 500 ml

Table 1: Components of the fixative and buffers.

Processing of Paraffin-Embedded Samples for Crossman's trichrome stain and immunohistochemical Staining

The fixed and decalcified specimens were dehydrated in an ascending series of ethanol Alcohol, cleared in methyl benzoate and then embedded in paraplast (Sigma Aldrich) (Table 2) showing the processing time of the samples in paraffin embedding techniques). Sequential longitudinal paraffin sections were obtained at 5-µm thickness, using a Richert Leica RM 2125 Microtome (Germany), and then the sections were stained by Crossman's trichrome stain [11]. The components of stains and method of stain shown in Table 3.

Processes	Time
Dehydration	
Alcohol70%I	24 h
Alcohol 70%II	12 h
Alcohol70%III	12h
Alcohol80%	1 h
Alcohol90%	1 h
Alcohol100%	1 h
Alcohol100%	1h
Clearing with methyl benzoate	
MBI	1d
MB II	1d
Embedding in paraffin	
P I	1h
P II	1h
PIII	2 h

Abbreviation: h, hours; d, days; MB I, methyl bonzoate1, MB II, methyl benzoate II; PI, paraffin I; P II, paraffin II; P III, paraffin III.
Table 2: The processing time of the samples in paraffin embedding techniques.

Solution A: Acid fuchsin Orange G	Acid fuchsin	1 g
	Orange G	400mg
	Distilled water	300ml
	Glacial acetic acid	3ml
Solution B (freshly prepared)	Phosphomolybdic or phosophtungsticacid	1 g
	Distilled water	100 g
Solution C: Light green	Light green	1 g
	Distilled water	100 ml
	Glacial acetic acid	1ml
Solution D: Glacial acetic acid	Glacial acetic acid	1 ml
	Distilled water	99 ml
Method	1-Deparafinization in xylene I and II for 20 minutes and hydrate in ethanol alcohol 100, 90, 80, 70% for 3 min in each concentration.	
	2- Rinse in distilled water	
	3- Rinse in distilled water stain in acid fuchsin Orange G for 1-5minutes	
	4- Rinse in a distilled water	
	5- Differentiate in 1% phosphomolybdic acid 5-10 minutes (until the red color disappear and the connective tissue becomes white).	
	6- Rinse in distilled water. Differentiate in 1% watery acetic acid (1 ml acetic acid+ 99 D.W) (until the green colour disappears from the muscles).	
	7- Stain in light green 1% for 5 minutes and then rinse in distilled water.	
	8- Differentiate in 1%watery acetic acid (until the green color disappears from the muscles).	
	9- Rinse in distilled water.	
	10- Dehydrate 3 times in 96% alcohol.	
	11- Dehydrate in 100% alcohol and then clear with xylene I, II	
	(Muscles become red, connective tissue becomes green and the nucleus becomes red).	
	12- Clear with xylene and cover using DPX.	

Table3: Crossomon's Stain preparations and method.

Immunohistochemical procedures of staining Matrix Metalloproteinase-9 (MMP-9)

We used mouse anti-rabbit antibody against matrix metalloproteinase-9 (MPP-9) for immunohistochemical staining. Immunostaining protocol was performed according to Soliman & Abd Elhafeez, [12], Soliman, Kamal & Abd Elhafeez [13], Mustafa & Elhanbaly [14], Soliman [15], Soliman & Madkour [16]. Antigen localization was achieved using mouse anti-rabbit antibody against matrix metalloproteinase-9 (MPP-9) combined with the avidin-biotin complex (ABC) technique Hsu, et al. [17]. We used the reagent of the Ultra-Vision Detection System [Anti-Polyvalent, HRP/DAB (ready to use, TP-015-HD: 15 mL Hydrogen Peroxide Block (TA-015-HP), 15 mL Ultra V Block (TA-015-UB), 15 mL Biotinylated Goat Anti-Polyvalent (TP-015-BN), 15 mL Streptavidin Peroxidase (TS-015-HR), 15 mL 3,3′-diaminobenzidine (DAB) Plus Substrate (TA-015-HSX), 1 mL DAB Plus Chromogen(TA-001-HCX), Thermo Fischer Scientific TP-015HD] according to the manufacturer's instructions. The procedure, according to the description of Abd Elhafeez, et al. [18], Mustafa & Elhanbaly [19] and was as follows: Paraffin sections of (5 µm) were dewaxed by xylene, rehydrated by ascending grades of alcohol and rinsed by PBS (Table 1) at a pH of 7.4(three times for 5 min). Endogenous peroxidase was suppressed by using a hydrogen peroxide block at room temperature. The sections were thoroughly washed by running tap water for an additional 10 min. Afterwards, to enhance antigen retrieval, the slides were treated with 10 mm sodium citrate buffer (Table 1) (pH 6.0) at a temperature of 95-98°C in a water bath for 20 min. The sections were cooled for 20 min at room temperature and

subsequently were washed in PBS (pH 7.4, three times for 5 min).

Blocking non-specific background staining was performed by using Ultra V block (Thermo Fisher Scientific, USA) for 5 min at room temperature. Ultra V block application did not exceed10 min to avoid staining artefacts. The primary antibody (Anti- MMP9 Thermo Fischer Scientific, Lab vision Corporation, Fremont, USA mMouse (mc, Ab-1) Clone D(33)376 RB-9423-PO Rabbit polyclonal, at dilution 1:30) was applied to sections overnight Sections were washed using PBS (at pH7.4, three times for 5 min). The biotinylated secondary antibody was applied for 10 min at room temperature. The biotinylated secondary antibody was Biotinylated goat Anti-Polyvalent Anti-mouse Igg + Anti -Rabbit Igg, Thermo Fisher Scientific, and, the UK Lab Vision Corporation; USA.

Sections were washed by PBS (pH 7.4, three times for 5 min) and subsequently incubated for 10 min at room temperature with the streptavidin– Peroxidase complex (Thermo Fisher Scientific, UK Lab Vision Corporation; USA). Visualization of the bound antibodies was performed using one drop of DAB plus chromogen to 2 mL of DAB plus substrate. The mixture was applied and incubated at room temperature for 5 min. The incubation processes were carried out in a humid chamber. Harris hematoxylin was used as a counterstain for 30 seconds. The sections were dehydrated using 95 %ethanol alcohol and isopropanol I and II, cleared in xylene and covered by DPX. Leitz Dialux 20 Microscope examined the stained sections. Photos were taken using Canon digital camera (Canon Power shot A95).

CMEIAS color segmentation (for the negative image)

Negative images were performed using CMEIAS Color Segmentation, a free download improved computing technology used to process color images by segmenting foreground object of interest from the background Gross, et al. [20]. This has been done according to description by Fatma M. Abdel-Masoud et al. Many authors used this technique in published paper [21-36].

Results

The distribution of MMP-9 expression by chondrocytes of articular cartilages of the 24 days embryos rabbit was detected. The articular cartilage of the immature rabbit consisted of chondrocytes (Figures 1A, B and Figures 2A-C) and surrounded by a peri-articular connective tissue or the perichondrium. The articular cartilage has grown by appositional growth that the chondroblasts or perichondrial stem cells differentiate into chondrocytes (Figures 1B and 2B).

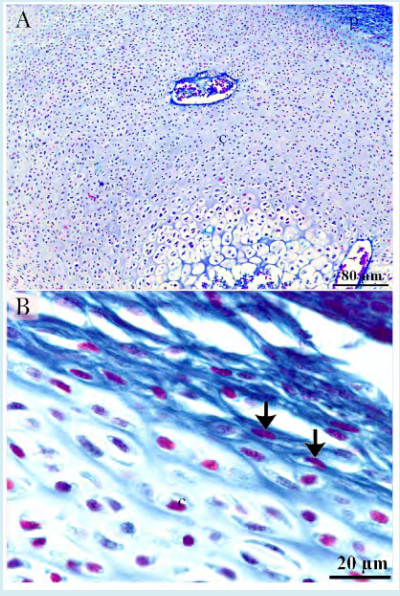

Figure 1: Paraffin sections articular cartilages of the femur at the 24-day rabbit of pregnancy stained by Mallory trichrome. A: Articular cartilage of the immature rabbit consisted of chondrocytes (C) and surrounded by peri-articular connective tissue or the perichondrium (p).B: Articular cartilage grown by appositional growth that the perichondrial stem cells (arrows) differentiate into chondrocytes (c).

Negative control of MMP-9 is seen in Figures 2(A-C). MMP-9 positive perichondrial stem cells (Figures 2 D-F, I) as well as chondroblasts and early chondrocytes (Figures 2F, I). Mature chondrocytes exhibited weak immunoaffinity for MMP-9 Figures 2G,H. Negative images of Figure 2 are seen in Supplementary Figure 3.

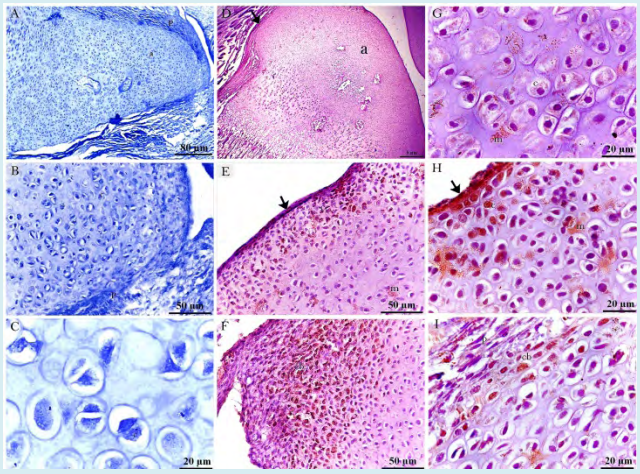

Figure 2: A distribution of MMP-9 in the articular cartilage of the embryonic rabbit femur Paraffin sections articular cartilages of the femur at the 24-day rabbit of pregnancy stained by with MMP-9 Immunohistochemical staining with MMP-9 (D-I) and negative control (A-C). A, B, C: Articular cartilage contained chondrocytes (c) and surrounded by perichondrium (p).D, E, H: Articular cartilage (a) surrounded by perichondrium that contained MMP-9 positive perichondrial stem cells (arrows) and differentiating chondrocytes (c).MMP-9 positive areas of cartilage matrix (m). G: mature chondrocytes (c) exhibited weak immunoaffinity for MMP-9. F, I: MMP-9 positive differentiating chondrocytes (c).

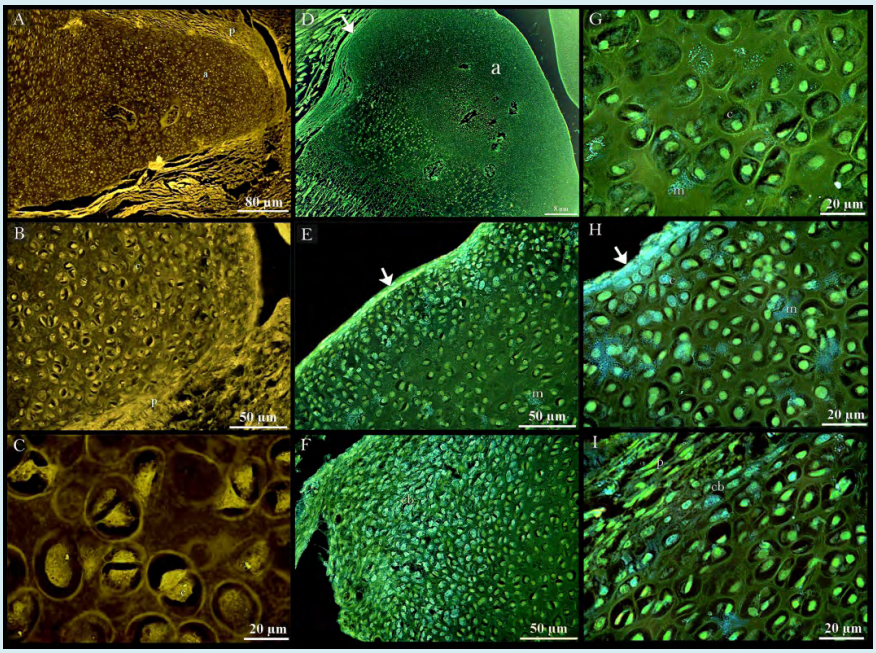

Figure 3: Negative image of figure 2 showing the distribution of MMP-9 in the articular cartilage of the embryonic rabbit femur Paraffin sections articular cartilages of the femur at the 24-day rabbit of pregnancy stained by with MMP-9 Immunohistochemical staining with MMP-9 (D-I) and negative control (A-C). A, B, C:Articular cartilage contained chondrocytes (c) and surrounded by perichondrium (p).D, E, H: Articular cartilage (a) surrounded by perichondrium that contained MMP-9 positive perichondrial stem cells (arrows) and differentiating chondrocytes (c). MMP-9 positive areas of cartilage matrix (m). G: mature chondrocytes (c) exhibited weak immunoaffinity for MMP-9. F, I: MMP-9 positive differentiating chondrocytes (c).

Discussion

The current results revealed transitory high expression of MMP-9 occurred during the early stages of chondrogenic differentiation. MMp-9 was strongly expressed in the chondroblasts or perichondrial stem cells or chondroblasts and differentiating chondrocytes while weak MMp-9 immunoaffinity was observed in mature chondrocytes. This indicates that chondroblasts and differentiating chondrocytes exhibited an active proteolytic stage and declining of the proteolytic activates occurred during chondrocyte maturation. With respect to that, the chondroblasts were small cell compared with the mature chondrocytes; we suggested that chondroblasts and differentiating chondrocytes degrade the cartilage in order to widen the lacunar space as that required for chondrocytes growth. Unlike other, study the results obtained by Cheng and his collages compare genes expression in articular cartilage and in dedifferentiated chondrocytes using qPCR. mRNA for matrix dedifferentiated chondrocytes (-). However, MMP-9 expression level is varied in different cartilages, including (temporomandibular joint condyle, femoral condyle, and tibial plateau) dissected from 1-month-old mice. The highest MMP-9 level is the femoral condyle, exceeding 5-fold higher compared to the temporomandibular joint condyle cartilage and 1.5-fold higher than in the tibial plateau cartilage. The MMP-9 activity in both the tibial plateau and femoral condyle in neonatal animals, during maturation and ageing is similar, unlike the temporomandibular joint condyle cartilage. A low level of MMP-9 has been detected in the tibial plateau and femoral condyle of the neonatal animals and elevates with the advancement of the animals' age. In contrast to the temporomandibular joint condyle cartilage, a high level of MMP-9 is determined during early growth (from 1 day to 2 weeks of age) and it declines during maturation and ageing [37]. Induction of MMP-9 expression in chondrocytes is regulated via the synergistic action of serum amyloid A-activating factors (SAF)-1, a transcription factor, and the AP-1 family of proteins [38]. Leptin enhances MMP-9 production by chondrocytes-induced IL-1β, via the PPAR-γ-independent mechanism [39].

Chondrocyte chondrolysis have been identified as degradation of the ECM components in the pericellular regions. Chondrocyte chondrolysis is a phenomenon that is recognized by losing of metachromatic affinity of the pericellular matrix of chondrocytes indicating depletion of proteoglycans. This phenomenon is associated with the appearance of matrix streaks that extending from the chondrocyte lacunae [40].

Chondrocytes have a dual function that secret and degrade matrix components by several enzymes including collagenase, neutral proteinases, and cathepsins [41]. Cartilage dynamics depends on both ECM secretion and degradation, which are strictly regulated to preserve the cartilage integrity. The imbalance between matrix secretion and degradation yields cartilage disorders. Chondrocytes could be enhanced to secrete MMP-1, MMP-2, MMP-3, MMP-7, MMP-9, MP-13, and MMP-14 16, ADAM- 9, ADAM-10, ADAM-17 as other proteolytic enzymes [42]. MMP-9 mRNA is estimated using reverse transcription-polymerase chain reaction (RT-PCR) in both osteoarthritic and normal cartilages. Higher levels of MMP-9 mRNA have been detected in osteoarthritic samples than in normal samples [43]. In rheumatoid arthritis, MMP-1, MMP-2, MMP-3, MMP-7, MMP-9, MMP-13, and MMP-14 are expressed by chondrocytes [42,44]. Osteoarthritic chondrocytes upregulate the expression of several extracellular matrix-degrading proteases particularly MMPs which target different extracellular matrix components. In osteoarthritic cartilage, the activity of the chondrolytic matrix metalloproteinases exceeds the anabolic activity of chondrocyte [45-50].

Conclusion

In the femoral articular cartilage of rabbit embryos, MMP-9 was strongly expressed by chondroblasts and early chondrocytes while mature chondrocytes exhibited weakly MMP-9 activity. We suggested that MMP-9 was essential during chondrocytes growth. The current study alludes to the potential role of MMP-9 during the growth of the articular cartilage.

References

1. Grassel S, Aszodi A (2107) Cartilage: Pathophysiology, Springer.

2. Stanton H, Melrose J, Little CB, Fosang AJ (2011) Proteoglycan degradation by the ADAMTS family of proteinases. Biochimica et Biophysica Acta (BBA) - Molecular Basis of Disease 1812(12): 1616-1629.

3. Cawston TE, Bigg H, Milner J, Catterall J, Morgan T, et al. (2005) Mechanisms of cartilage matrix turnover: synergistic interactions of proinflammatory cytokines with oncostatin M in upregulating matrix metalloproteinases and ADAMTS metalloproteinases. Arthritis Research & Therapy 7(1): 10-10.

4. Soder S, Roach HI, Oehler S, Bau B, Haag J, et al. (2006) MMP-9/gelatinase B is a gene product of human adult articular chondrocytes and increased in osteoarthritic cartilage. Clin Exp Rheumatol 24(3): 302-304.

5. Wrobel KH, Moustafa MN (2000) On the innervation of the donkey testis. Ann Anat 182(1): 13-22.

6. Moustafa MNK, Sayed R, Zayed AE, AbdEl Hafeez HH (2015) Morphological and morphometric study of the development of seminiferous epithelium of donkey (Equus asinus) from birth to maturity. J Cytol Histol 6(6): 1.

7. Abd Elhafeez H, Moustafa K, Zayed AE, Sayed R (2017) Morphological and Morphometric Study of the Development of Leydig Cell population of Donkey (Equus asinus) Testis from Birth to Maturity. Cell Biology: Research & Therapy 6(1): 2.

8. Abd-Elhafeez HH, Moustafa MN, Zayed AE, Sayed R (2017) The development of the intratesticular excurrent duct system of donkey (*Equus asinus*) from birth to maturity. Histol Cytol Embryol 1(2): 6-8.

9. Abdel-latief Soliman SM, Ali Emeish WF (2017) Morphological Alternations of Intraepithelial and Stromal Telocytes in Response to Salinity Challenges. bioRxiv pp: 115881.

10. Roach HI (1997) New Aspects of Endochondral Ossification in the Chick: Chondrocyte Apoptosis, Bone Formation by Former Chondrocytes, and Acid Phosphatase Activity in the Endochondral Bone Matrix. Journal of Bone and Mineral Research 12(5): 795-805.

11. Suvarna K, Layton C, Bancroft J (2013) Bancroft's Theory and Practice of Histological Techniques. 7th (Edn.), Elsevier Churchill Livingstone.

12. Soliman SA, Abd-Elhafeez HH (2016) Are C-KIT, MMP-9 and Type II Collagen Positive Undifferentiated Cells Involved in Cartilage Growth? A Description of Unusual Interstitial Type of Cartilage Growth. J Cytol Histol 7: 440.

13. Soliman SA, Kamal BM, Abd-Elhafeez HH (2019) Cellular invasion and matrix degradation, a different nature of matrix degrading-cells in the cartilage of catfish (Clarias gariepinus) and Japanese Quailembryos (Coturnix coturnix japonica). Microsc.Microanal 25(5): 1283-1292.

14. Mustafa FEZ, Elhanbaly R (2020) Distribution of estrogen receptor in the rabbit cervix during pregnancy with special reference to stromal elements: an immunohistochemical study 10. Scientific Reports 10: 13655.

15. Soliman SA (2021) Telocytes are major constituents of the angiogenic apparatus. Scientific Reports 11(1): 5775.

16. Soliman SA, Madkour FA (2021) Developmental events and cellular changes occurred during esophageal development of quail embryos. Scientific Reports 11(1): 7257.

17. Hsu SM, Raine L, Fanger H (1981) Use of avidin-biotin-peroxidase complex (ABC) in immunoperoxidase techniques: a comparison between ABC and unlabeled antibody (PAP) procedures. The journal of histochemistry and cytochemistry 29(4): 577-580.

18. Abd-Elhafeez HH, Abdo W, Kamal BM, Soliman SA (2020) Fish telocytes and their relation to rodlet cells in ruby-red-fin shark (rainbow shark) Epalzeorhynchos frenatum (Teleostei: Cyprinidae). Scientific Reports 10(1): 18907.

19. Mustafa FEZA, Elhanbaly R (2020) Histological, histochemical, immunohistochemical and ultrastructural characterization of the testes of the dove. Zygote pp: 1-9.

20. Gross CA, Reddy CK, Dazzo FB (2010) CMEIAS color segmentation: an improved computing technology to process color images for quantitative microbial ecology studies at single-cell resolution. Microbial ecology 59(2): 400-414.

21. Soliman SA, Ahmed YA, Abdelsabour-Khalaf M (2016) Histogenesis of the stomach of the pre-hatching quail: a light microscopic study. Anatomical Science International 91(4): 407-418.

22. Abd-Elkareem M (2017) Cell-specific immuno-localization of progesterone receptor alpha in the rabbit ovary during pregnancy and after parturition. Animal reproduction science 180: 100-120.

23. Soliman S (2017) Potential Role of Telocytes in Development of Embryonic Ganglia. SF J Stem Cell 1(1): 1.

24. Soliman SA (2017) Telocytes during organogenesis: Relations to nephrogenic cords in mesonephros of quail embryos. Histol Cytol Embryol 1(4): 1-6.

25. Soliman SA, Hassan H, Enas A (2017) A new mechanism of cartilage growth in mammals ''involvement of CD117 positive undifferentiated cells in interstitial growth. MJ Cyto 1(1): 001.

26. Soliman S (2017) Potential Role of Telocytes in Differentiation of Embryonic Skeletal Progenitor Cells. SF J Stem Cell 1(1).

27. Ibrahim D, Gaber W, Awad M (2018) Temporospatial localization of telocytes during esophageal morphogenesis in rabbit. Acta histochem 121(1): 64-71.

28. Soliman AS (2018) The growth cartilage and beyond:

Absence of medullary bone in silver carp ribs. Mathew J Cytol Histol 2(1): 008.

29. Abd-Elkareem M, Abou-Elhamd AS (2019) Immunohistochemical localization of progesterone receptors alpha (PRA) in ovary of the pseudopregnant rabbit. Animal Reproduction 16(2): 302-310.

30. Abdel-Hakeem SS, Mahmoud G, Abdel-Hafeez H (2019) Evaluation and Microanalysis of Parasitic and Bacterial Agents of Egyptian Fresh Sushi, Salmo salar. Microsc Microanal 25(6): 1498-1508.

31. Mustafa FA (2019) Putative primo-vascular system in rabbit placenta. J Acupunct Meridian Stud 12(1): 20-24.

32. Soliman SA (2019) Morphological and histochemical description of quail feather development. Anat. Rec.

33. Yousef MS, Abd-Elhafeez HH, Talukder AK, Miyamoto A (2019) Ovulatory follicular fluid induces sperm phagocytosis by neutrophils, but oviductal fluid around oestrus suppresses its inflammatory effect in the buffalo oviduct in vitro. Mol Reprod Dev 86(7): 835-846.

34. Abd-Elhafeez HH, Abou-Elhamd AS, Soliman SA (2020) Morphological and immunohistochemical phenotype of TCs in the intestinal bulb of Grass carp and their potential role in intestinal immunity. Sci Rep 10: 14039.

35. Abd-Elhafeez HH, Abou-Elhamd AS, Abdo W, Soliman SA (2020) Migratory Activities and Stemness Properties of Rodlet Cells. Microscopy and Microanalysis pp: 1-18.

36. Abd-Elhafeez H, Hassan A, Hussein MM (2021) Melatonin administration provokes the activity of dendritic reticular cells in the seminal vesicle of Soay ram during the non-breeding season. Scientific Reports pp: 11.

37. Gepstein A, Shapiro S, Arbel G, Lahat N, Livne E (2002) Expression of matrix metalloproteinases in articular cartilage of temporomandibular and knee joints of mice during growth, maturation, and aging. Arthritis Rheum 46(12): 3240-3250.

38. Ray A, Bal BS, Ray BK (2005) Transcriptional induction of matrix metalloproteinase-9 in the chondrocyte and synoviocyte cells is regulated via a novel mechanism: evidence for functional cooperation between serum amyloid A-activating factor-1 and AP-1. J Immunol 175(6): 4039-4048.

39. Ardani PG, Kalim H, Indra R (2017) Leptin Increase Matrix Metalloproteinase-9 (MMP-9) Secretion By Chondrocytes-Induced IL-1β, Through PPAR-γ Suppression. Imperial Journal of Interdisciplinary Research 3(2): 2454-1362.

40. Kuettner KE (1992) Articular Cartilage and Osteoarthritis, Raven Press.

41. Cassidy JT, Petty RE, Ronald M, Lindsley CB (2010) Textbook of Pediatric Rheumatology E-Book: Expert Consult: Online and Print, Elsevier Health Sciences.

42. Firestein GS, Budd R, Gabriel SE, McInnes LB, O Dell JR (2012) Kelley's Textbook of Rheumatology E-Book, Elsevier Health Sciences.

43. Matoney WJ, Vu T, Hoffman AR, Schurman DJ, Smith RL (1996) RT-PCR Analysis of MMP-9 Expression in Human Articular Cartilage Chondrocytes and Synovial Fluid Cells AU - Tsuchiya, K. Biotechnic & Histochemistry 71(4): 208-213.

44. Freemont A, Hampson V, Tilman R, Goupille P, Taiwo Y, et al. (1997) Gene expression of matrix metalloproteinases 1, 3, and 9 by chondrocytes in osteoarthritic human knee articular cartilage is zone and grade specific. Ann Rheum Dis 59(9): 542-549.

45. Aigner T, Schmitz N, Salter DM (2014) Pathogenesis and pathology of osteoarthritis.

46. Abdel Maksoud FM, Abd Elhafeez HH, Soliman SA (2019) Morphological changes of telocytes in camel efferent ductules in response to seasonal variations during the reproductive cycle. Sci Rep 9(1): 1-17.

47. Cheng T, Maddox NC, Wong AW, Rahnama R, Kuo AC (2012) Comparison of gene expression patterns in articular cartilage and dedifferentiated articular chondrocytes. J Orthop Res 30(2): 234-245.

48. Grassel S, Aszodi A (2107) Cartilage: Pathophysiology, Springer.

49. Soliman SA, Abd-Elhafeez HH (2016) Mesenchymal Cells in Cartilage Growth and Regeneration An Immunohistochemical and Electron Microscopic Study. J Cytol Histol 7: 437.

50. Soliman SA, Madkour FA (2017) A comparative analysis of the organization of the sensory units in the beak of duck and quail. Histology, Cytology and Embryology 1(4): 2-16.